arXiv:1609.03483v1 [cond-mat.stat-mech] 12 Sep 2016

Generalized Thermodynamics of Phase Equilibria in Scalar Active Matter

Alexandre P. Solon,[1] Joakim Stenhammar,[2] Michael E. Cates,[3] Yariv Kafri,[4] and Julien Tailleur[5]

[1] *Massachusetts Institute of Technology, Department of Physics, Cambridge, Massachusetts 02139, USA*
[2] *Division of Physical Chemistry, Lund University, 221 00 Lund, Sweden*
[3] *DAMTP, Centre for Mathematical Sciences, University of Cambridge, Cambridge CB3 0WA, United Kingdom*
[4] *Department of Physics, Technion, Haifa, 32000, Israel*
[5] *Université Paris Diderot, Sorbonne Paris Cité, MSC, UMR 7057 CNRS, 75205 Paris, France*

(Dated: September 13, 2016)

Motility-induced phase separation (MIPS) arises generically in fluids of self-propelled particles when interactions lead to a kinetic slowdown at high density. Starting from a continuum description of diffusive scalar active matter, we give a general prescription for phase equilibria that amounts, at a hydrodynamics scale, to extremalizing a generalized free energy. We illustrate our approach on two well known models: self-propelled particles interacting either through a density-dependent propulsion speed or via direct pairwise forces. Our theory accounts quantitatively for their phase diagrams, providing a unified description of MIPS, and explains their qualitatively different behavior when changing ensembles from isochoric to isobaric.

PACS numbers: 05.40.-a; 05.70.Ce; 82.70.Dd; 87.18.Gh

Active materials, composed of particles individually capable of dissipatively converting energy into motion, display a fascinating range of large-scale properties [1–6]. Commonly found in nature but also engineered in the lab [7–11], they attract interest both for their foreseeable applications in directed assembly [12] and for the challenges they pose to statistical mechanics. Motility-induced phase separation [13] (MIPS) is a characteristic phenomenon of active matter which has attracted lots of interest recently [11, 13–28]. It arises because self-propelled particles accumulate in regions where they move more slowly [29]. When interactions between particles lead to their slowing down at high density, a positive feedback leads to phase separation between a high-density low-motility phase and a low-density high-motility phase. Remarkably, this liquid-gas phase-separation happens without the need of any attractive interactions, leading to the emergence of cohesive matter without cohesive forces. First postulated in idealized toy models [14–20], MIPS has since been addressed experimentally using self-propelled colloids [11, 21] and genetically engineered bacteria [30].

Although MIPS share similarities with an equilibrium liquid-gas transition in both the shape of its phase diagram [17] and its coarsening dynamics [15, 19], there is currently no working theory to predict its phase equilibria. Interestingly, the thermodynamic relations that constrain the coexisting phases in equilibrium are violated in MIPS in a system-dependent fashion. In a first class of models [14, 15, 31], MIPS arises from an explicit density-dependence of the propulsion speed $v(\rho)$. This mimics the way bacteria or cells adapt their motion to the local density measured through the local concentration of a chemical signal, and we refer to such particles as 'quorum-sensing' active particles (QSAPs). These models can be mapped at the diffusion-drift level onto an equilibrium system. This allows to define a chemical potentials μ which is equal in coexisting gas and liquid phases [14, 32]. This mapping however breaks down at higher order in gradients, such that the coexisting pressures P, whether mechanical [33] or thermodynamic [22], are unequal. In a second class of scalar models [16–19], particles with constant propulsion speed interact via isotropic pairwise forces (no alignment interactions); the slowdown triggering MIPS is now due to collisions. Contrary to QSAPs, the mechanical pressure of such 'pairwise-force active particles' (PFAPs), defined as the force density on a confining wall, is equal in coexisting phases. (This is a signature of an underlying equation of state for P in PFAPs [23, 28, 34].) However, a chemical potential defined from the thermodynamic equilibrium relation [35] $P = N\mu - F$ with $\partial F/\partial N = \mu$ would take unequal values in coexisting phases, causing violation of the equilibrium Maxwell (equal area) construction [28]. All in all, despite the frequently-highlighted similarities between PFAPs and QSAPs [16, 18, 28, 32], a comprehensive theory of MIPS remains elusive.

In this Letter, we propose such a unified theory, based on continuum-level, hydrodynamic equations of motion for the scalar density field (without momentum conservation). We show how active phase equilibria obey at this level a common tangent construction on a generalized free energy density. Our formalism encompasses equilibrium systems for which one recovers the standard thermodynamic free energy and, in that case only, the equality among phases of both pressure and chemical potential. Our theory not only accounts quantitatively for MIPS phase diagrams, but also explains the contrasting manners in which the equilibrium relations are violated in QSAPs and PFAPs. Furthermore, we show how this difference plays a crucial role when changing ensemble, which we illustrate for the case of an isobaric construc-

tion.

General framework. We consider a continuum description of active particles with isotropic, non-aligning interactions. The sole hydrodynamic field is thus the conserved density $\rho(\mathbf{r},t)$, obeying $\dot\rho=-\nabla\cdot\mathbf{J}$. By symmetry, the current $\mathbf{J}$ vanishes in homogeneous phases. Its expansion in gradients of the density involves only odd terms under space reversal so we can assume that, at dominant order, $\mathbf{J}$ is parallel to density gradients:

$$\dot\rho=-\nabla\cdot(M\nabla g);\ g=g_0(\rho)+\lambda(\rho)|\nabla\rho|^2-\kappa(\rho)\Delta\rho. \quad (1)$$

Here the mobility M is an arbitrary functional of ρ [36] which, rather surprisingly outside equilibrium, turns out not to play any role in the phase equilibrium. The noiseless 'hydrodynamic' equation (1) describes the evolution of the average density field on length and time scales much larger than the correlation length and time.

We now establish the general phase equilibria predicted by Eq. (1) before turning to specific models. Consider a fully phase-separated system with coexisting gas and liquid phases at densities ρ_g and ρ_ℓ. In a steady state with vanishing mass current, $M\nabla g=0$, so that g is constant throughout the system: $g[\rho(r,t)]=\bar g$. This yields a first equation relating ρ_g and ρ_ℓ:

$$g_0(\rho_g)=g_0(\rho_\ell)=\bar g. \quad (2)$$

In the macroscopic limit, interfaces are effectively flat; we thus consider an interface between the phases localized at $x=0$, parallel to $\hat{\mathbf{y}}$ [37]. A second relation can now be obtained by integrating $g(\rho)\partial_x R$ across the interface, with $R(\rho)$ an arbitrary function of ρ. Replacing $g(\rho)$ by its value $\bar g$ or its explicit expression in Eq. (1), one finds two equivalent expressions for $\int_{x_g}^{x_\ell} g(\rho)\partial_x R\,dx$:

$$\bar g(R_\ell-R_g)=\phi(R_\ell)-\phi(R_g)+\int_{x_g}^{x_\ell}[\lambda(\partial_x\rho)^2-\kappa\partial_x^2\rho]\partial_x R\,dx \quad (3)$$

where x_g and x_ℓ lie within the bulk gas and liquid phases, $R_{\ell/g}\equiv R(\rho_{\ell/g})$, and ϕ is defined by $d\phi/dR=g_0(\rho)$.

Since $R(\rho)$ is arbitrary, we can choose it to make the integral in Eq. (3) vanish. Indeed, if R satisfies $R''=-(2\lambda+\kappa')R'/\kappa$, where $(')$ denotes $d/d\rho$, we have

$$[\lambda(\partial_x\rho)^2-\kappa\partial_x^2\rho]\partial_x R=-\partial_x\left[\frac{\kappa R'}{2}(\partial_x\rho)^2\right] \quad (4)$$

whose integral vanishes between any two bulk planes with $\partial_x\rho=0$. Eq. (3) therefore yields a second constraint:

$$h_0(R_\ell)=h_0(R_g);\qquad h_0(R)\equiv R\phi'(R)-\phi(R) \quad (5)$$

Eqs. (2,5) show the coexisting densities to satisfy a common tangent construction on a transformed (bulk) free energy $\phi(R)=\int g_0(\rho)dR$. Because R is nonlinear in ρ, the lever rule, $\rho_\ell V_\ell+\rho_g V_g=\rho V$ is nonlinear in R, but still determines the phase volumes $V_{\ell,g}$. Also the densities $\rho_{\ell,g}$ do not vary as one moves along the 'tie-line' by changing the global mean density ρ. This is not true generally in non-equilibrium phase separation [38], but is a consequence of our transformed free-energy structure.

We discuss these results first for systems where

$$g=\frac{\delta\mathcal{F}}{\delta\rho(x)};\quad \mathcal{F}[\rho]=\int[f(\rho)+\frac{c(\rho)}{2}(\nabla\rho)^2]dx \quad (6)$$

Eq. (1) is then simply the Cahn-Hilliard equation [39] for a system with free energy $\mathcal{F}[\rho]$ and mobility $M[\rho]$. Eq. (6) then imposes $2\lambda+\kappa'=0$ so that $R''=0$. Choosing $R=\rho$, we recover $\phi(R)=f(\rho)$ as the bulk free energy density, $g_0(\rho)=f'(\rho)$ as the chemical potential, and $h_0(\rho)=f'(\rho)\rho-f(\rho)$ as the thermodynamic pressure.

Our transformed common tangent construction thus reverts to the usual one in equilibrium systems, where it is equivalent to globally minimizing $\mathcal{F}$. Outside equilibrium, when no $\mathcal{F}$ exists and the steady-state distribution is unknown, g can always be written at hydrodynamic level as $g(x)=\frac{\delta\mathfrak{F}}{\delta R(x)}$, with $\mathfrak{F}=\int d\mathbf{r}[\phi(R)+\frac{\kappa}{2R'}(\nabla R)^2]$. The dynamics (1) then leads to extrema of the transformed functional free-energy landscape $\mathfrak{F}$ which explains why conditions (2,5) are structurally reminiscent of the equilibrium case. It however extends outside equilibrium (see SI for numerical illustrations [40]) and includes the two microscopic models of MIPS introduced above.

QSAPs. We consider particles $i=1....N$, moving at speeds v_i along body-fixed directions $\mathbf{u}_i$, which undergo both continuous rotational diffusion with diffusivity D_r and complete randomization with tumbling rate α. Each particle adapts its speed $v(\tilde\rho_i)$ to its local density

$$\tilde\rho_i(\mathbf{r})=\int d\mathbf{r}'K(\mathbf{r}+\varepsilon\mathbf{u}_i-\mathbf{r}')\hat\rho(\mathbf{r}')d\mathbf{r}' \quad (7)$$

with $K(\mathbf{r})$ an isotropic coarse-graining kernel, and $\hat\rho(\mathbf{r})=\sum_i\delta(\mathbf{r}-\mathbf{r}_i)$ the microscopic particle density. The term in ε optionally allows for anisotropic (e.g., visual) quorum sensing; it does not create alignment interactions.

Deriving hydrodynamic equations from microscopics is generally difficult, even in equilibrium [41]. For QSAPs we can follow the path of [14, 32, 42], taking a mean-field approximation of their *fluctuating* hydrodynamics. We first assume a smooth density field and a short-range anisotropy so that the velocity can be expanded as [40]

$$v(\tilde\rho_i)\approx v(\rho)+\varepsilon v'(\rho)\nabla\rho\cdot\mathbf{u}_i+\ell^2 v'(\rho)\Delta\rho+\mathcal{O}(\varepsilon^2,\nabla^3) \quad (8)$$

where ρ is evaluated at $\mathbf{r}_i$ and $\ell^2=\int r^2K(\mathbf{r})d\mathbf{r}$. Following [32, 42], the fluctuating hydrodynamics of QSAPs is then given by $\dot\rho=-\nabla\cdot(M\nabla g+\sqrt{2M\rho}\mathbf{\Lambda})$ [40], with $\mathbf{\Lambda}$ a unit white noise vector and

$$\begin{aligned} g_0(\rho)&=\log(\rho v)+\frac{\varepsilon}{\tau v};\quad M=\rho\frac{\tau v(\tilde\rho)^2}{d},\\ \kappa(\rho)&=-\ell^2\frac{v'}{v}(1-\frac{\varepsilon}{\tau v});\quad \lambda(\rho)=0. \end{aligned} \quad (9)$$

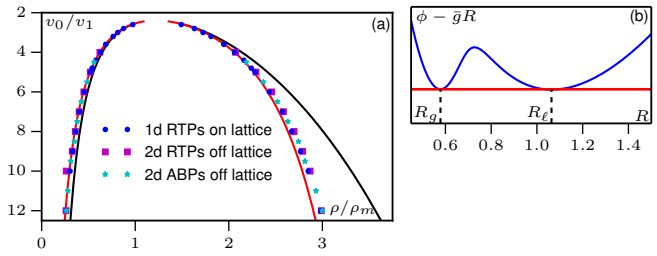

Figure 1. **a**: Phase diagrams of QSAPs. The solid lines correspond to common tangent constructions on $\phi(R)$ (red) or $f(\rho)$ (black). Data points are from 1d or 2d simulations run-and-tumble particles (RTPs, $\alpha = 1$, $D_r = 0$) or active Brownian particles (ABPs, $\alpha = 0$, $D_r = 1$) in continuous space or on lattice. For all plots, $v(\rho) = v_0 + \frac{v_1 - v_0}{2}\left[1 + \tanh(\frac{\rho - \rho_m}{L_f})\right]$, $K(r) = \exp(-\frac{1}{1-r^2})/Z$ with Z a normalization constant, $\rho_m = 200$, $v_1 = 5$, $L_f = 100$, $\varepsilon = 0$. **b**: Common tangent construction on $\phi(R)$ for $v_0 = 20$, $\varepsilon = 0$.

Here, $\tau = [(d-1)D_r + \alpha]^{-1}$ is the orientational persistence time. The mean-field hydrodynamic equation of QSAPs is then Eq. (1) with the coefficients in Eq. (9).

Inspection of these coefficients shows that $2\lambda + \kappa' \neq 0$ and hence $R \neq \rho$ [19, 22]. Thus the phase diagram cannot be found by globally minimizing a free energy density $f(\rho)$ such that $f'(\rho) = g_0(\rho)$ [14, 32]. Instead, for a given choice of $v(\rho)$, we first solve for $R(\rho)$ and from it obtain both $\phi(R)$ and $h_0(R)$. The binodals then follow via a common-tangent construction on $\phi(R)$ or, equivalently, by setting equal values of h_0 and g_0 in coexisting phases.

Fig. 1 shows the phase diagrams predicted by our generalized thermodynamics and by QSAP simulations. Since our derivation of Eq. (1) relies on a mean-field approximation, we choose a $v(\rho)$ such that MIPS occurs only at large densities [40]. As expected, the hydrodynamic equation works best fairly close to the critical point which at these densities remains mean-field like (modulo a small and numerically unresolved Ginzburg interval). This is where interfaces are smoothest and the gradient expansion Eq. (8) most accurate; the asymmetry ε also has to be small compared to the interface width [40]. These quantitative limitations of square gradient theory remind us that *nonlocal terms directly influence the phase diagram* (cf. [43]) – quite unlike the equilibrium case. Nonetheless, the agreement between predicted and measured binodals is excellent, in contrast to the common tangent construction on $f(\rho)$. It is remarkable that for QSAPs we can quantitatively predict the phase diagram of a microscopic model without any fitting parameter, something rare even for equilibrium models.

Beyond the quantitative prediction of the phase diagrams, our approach provides insight into the universality of the MIPS seen for QSAPs. For instance, the phase diagram does not depend on the details of the kernel K, which enters Eq. (9) only through ℓ^2 which then cancels in the nonlinear transform $R(\rho)$. Likewise, Fig. 1 includes lattice simulations of QSAPs in $1d$ where full phase separation is replaced by alternating domains (whose densities obey the predicted binodal values), and confirms the equivalence of continuous (ABP) and discrete (RTP) angular relaxation dynamics for QSAPs [32, 42]. However, our results also expose sensitivity to other microscopic parameters such as the fore-aft asymmetry ε which enters g_0 and hence directly affects the binodals [40]. This could explain the different collective behaviors seen in swarms of robots that adapt their speeds to the density sampled in either the forward or the backward direction [44].

PFAPs. We now consider self-propelled particles, of diameter σ, in $2d$, interacting via a short-range repulsive pair potential V (see [40] for details):

$$\dot{\mathbf{r}}_i = -\sum_j \nabla_i V(|\mathbf{r}_i - \mathbf{r}_j|) + \sqrt{2D_t}\boldsymbol{\xi}_i + v\mathbf{u}_i;\ \dot{\theta}_i = \sqrt{2D_r}\eta_i.$$

Here a microscopic mobility multiplying the first term was set to unity; $\mathbf{u}_i = (\cos\theta_i, \sin\theta_i)$, and $\eta_i, \boldsymbol{\xi}_i$ are unit Gaussian white noises. For simplicity, we only include continuous rotational diffusion, but our results straightforwardly extend to allow for tumbles. MIPS occurs in this system if the Péclet number $\mathrm{Pe} = 3v_0/(\sigma D_r)$ exceeds a threshold value $\mathrm{Pe}_c \sim 60$ [16–19].

Following [28, 45], we derive in [40] a fluctuating hydrodynamics for the stochastic density $\hat{\rho}(\mathbf{r}) = \sum_{i=1}^N \delta(\mathbf{r} - \mathbf{r}_i)$ whose deterministic limit gives a coarse-grained equation for the mean density field. On time scales larger than D_r^{-1}, in our phase-separated set-up with a flat interface parallel to $\hat{\mathbf{y}}$, this leads to $\dot{\rho} = \partial_x^2 g$, with

$$\begin{aligned} g([\rho], x) &= D_t\rho + \frac{v^2}{2D_r}(\rho + m_2) + \hat{I}_2 - \frac{v_0 D_t}{D_r}\partial_x m_1 + P_D \\ P_D &= \int_{-\infty}^{x} dx \int \partial_x V(\mathbf{r}' - \mathbf{r})\langle\hat{\rho}(\mathbf{r}')\hat{\rho}(\mathbf{r})\rangle d^2\mathbf{r}' \qquad (10) \\ \hat{I}_2 &= -\frac{v}{D_r}\int \partial_x V(\mathbf{r}' - \mathbf{r})\langle\hat{\rho}(\mathbf{r}')\hat{m}_1(\mathbf{r})\rangle d^2\mathbf{r}' \end{aligned}$$

Here, $\hat{m}_n = \sum_{i=1}^N \delta(\mathbf{r} - \mathbf{r}_i)\cos(n\theta_i)$ and $m_n = \langle\hat{m}_n\rangle$, where $\langle\dots\rangle$ represent averages over noise realizations. The lack of steady-state current shows g to be uniform in the phase-separated system, equal to some constant $\bar{g}$.

Remarkably, for homogeneous systems the expression for g in Eq. (10) reduces exactly to the equation of state (EOS) found previously for the mechanical pressure P of PFAPs [28]. Thus g is equal between phases, as it was for QSAPs, but now it represents pressure, not chemical potential. Moreover, Eq. (10) generalizes the pressure EOS of [28] to inhomogeneous situations. It can formally be written $g = g_0(\rho(x)) + g_{\mathrm{int}}([\rho], x)$ where $g_0(\rho)$ is the pressure in a notionally homogeneous system of density ρ, and the 'interfacial' term g_{int} represents all nonlocal corrections to this. The form of g used in Eq. (1) can then for PFAPs be viewed as a gradient expansion of Eq. (10).

One way forward would be to make that expansion (or perhaps avoid it by using a closed-form ansatz for g_{int}),

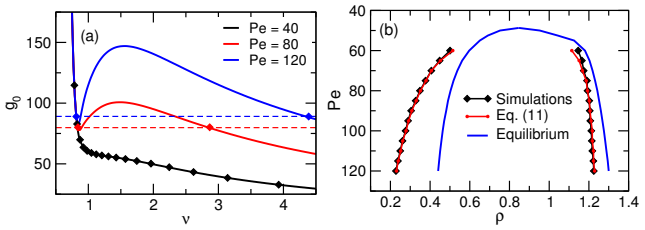

Figure 2. **a**: Semi-empirical EOS for the mechanical pressure $g_0(\nu)$ for various Pe. Horizontal lines correspond to the pressure $\bar{g}$ predicted by Eq. (11). **b**: Corresponding phase diagrams obtained via the modified (red; see text) and the equal-area (blue) Maxwell constructions, compared with numerically measured binodals (black).

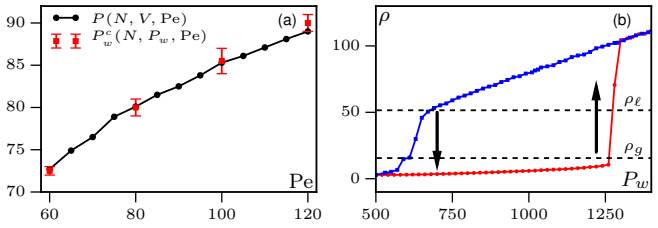

Figure 3. Simulations in the isobaric N, P_w, Pe ensemble. **a**: For each Péclet number the phase transition (red) occurs when the imposed pressure equals the mechanical pressure of coexisting gas and liquids in the isochoric ensemble (black). **b**: For QSAPs, the volume is not single-valued in the imposed mechanical pressure P_w, leading to large hysteresis loops.

and then find $R(\rho)$ and $\phi(R)$ analytically as was done for QSAPs above. Here however we proceed differently, approximating instead the local part, $g_0(\rho)$, of g in Eq. (10) by a well benchmarked, semi-empirical EOS, with parameters constrained by simulations of uniform phases at $\mathrm{Pe} = 40 < \mathrm{Pe}_c$ [40]. We thus retain the *exact structure* of the nonlocal terms, $g_{\rm int}(x) \equiv g([\rho], x) - g_0(\rho(x))$ in Eq. (10), but find them numerically. Although less predictive than knowing such terms algebraically, our method clearly illustrates how they select the binodals.

We proceed as in Eq. (3) but with R now chosen as the volume per particle $\nu \equiv \rho^{-1}$. The integral $\int_{x_g}^{x_\ell}(g - g_0)\,\partial_x\nu\,dx$ then admits two equivalent expressions

$$\int_{\nu_\ell}^{\nu_g} (g_0(\nu) - \bar{g}) d\nu = \int_{x_g}^{x_\ell} g_{\rm int}\,\partial_x\nu\,dx. \qquad (11)$$

Here $g_0(\nu)$ is the pressure-volume EOS, so the non-zero value of the right hand integral *directly* quantifies violation of the Maxwell construction. A fully predictive theory would evaluate the right hand side integral and then solve $g_0(\nu_\ell) = g_0(\nu_g) = \bar{g}$ together with Eq. (11) to obtain the values of the binodals ν_ℓ and ν_g. In practice, we measure $g_{\rm int}(x)$ numerically via Eq. (10) from which we subtract $g_0(\rho(x))$. The right hand side of Eq. (11) is then held constant at its numerically determined value. Crucially, $\bar{g}$, ν_g and ν_ℓ are not inputs here, but are found via a modified Maxwell construction: The binodals correspond to the intersect between the function $g_0(\nu)$ and a horizontal line of (unknown) ordinate $\bar{g}$ since $g_0(\nu_\ell) = g_0(\nu_g) = \bar{g}$. The value of $\bar{g}$ can then be set to satisfy Eq. (11). This construction is illustrated in Fig. 2, and is accurately obeyed by simulations, unlike the equilibrium Maxwell construction, which (notwithstanding [35]) clearly fails to account for the phase equilibria of PFAPs where nonlocal terms again directly enter.

Ensembles. One powerful aspect of equilibrium thermodynamics is that it relates the physical states of a system under different environmental constraints. Beyond its engineering value, the existence of several ensembles provides useful theoretical tools to study phase transitions [46]. Similar developments for non-equilibrium systems have however proven difficult [47–49]. Interestingly, our generalized thermodynamics allows some progress.

We adapt our previous constant volume (isochoric) simulations to consider an isobaric (constant pressure) ensemble. PFAPs or QSAPs are now confined by mobile harmonic walls, subject to a constant force density P_w which imposes a mechanical pressure $P = P_w$. Since $P = g_0$ is a generalized thermodynamic variable for PFAPs, we expect, as in equilibrium, that the coexistence *region* of the isochoric (N, V, Pe) ensemble collapses onto a coexistence *line* in the isobaric (N, P, Pe) case, corresponding to the pressure at coexistence in the isochoric ensemble. This is confirmed in Fig 3a. In contrast, for QSAPs the mechanical pressure P is unrelated to either of the generalized variables g_0, h_0. The same value of P_w may thus lead to different states of the system depending on its history: the Gibbs phase rule does not apply for QSAPs in this ensemble. This translates into large hysteresis loops when slowly cycling P_w, as shown in Fig 3b.

In this Letter, we have shown how to build a generalized thermodynamics of phase-separating scalar active matter, starting from hydrodynamic-level expressions for the density current. Our work accounts for the phase equilibria of two important classes of self-propelled particles, PFAPs and QSAPs, which each undergo MIPS. In contrast to equilibrium systems, nonlocal contributions to pressure and/or chemical potential generically determine the binodal densities at coexistence [22, 28]. We have given in Eqs. (2,5) an *explicit construction* for the binodals at the square gradient level of nonlocality. This is quantitatively accurate for MIPS in QSAPs at high density. In Eq. (11) we have given a more general construction that holds beyond the gradient expansion; we tested it using numerical data on PFAPs.

Interestingly, QSAPs and PFAPs share the same mathematical structure but with different interpretation of the variable g whose gradient drives the particle current. For QSAPs, g is viewed as chemical potential; for PFAPs, g is mechanical pressure. Spatial uniformity of g provides one coexistence condition; this is immune to gradient terms (which vanish in both bulk phases). The second con-

dition involves nonlocal terms, leading to a violation of the common tangent construction for QSAPs and the Maxwell construction for PFAPs. These violations vanish only when the nonlocality is of equilibrium form.

Our identification of the relevant intensive variables is important both for understanding the phase equilibria of active matter and to properly define thermodynamic ensembles, which we have illustrated by considering the isobaric ensemble for QSAPs and PFAPs. We hope that our approach will pave the way towards a more general definition of intensive thermodynamic parameters [47–49] for active matter, which would further improve our understanding and control of these intriguing systems.

Acknowledgements: We thank M. Kardar, H. Touchette for discussions. APS acknowledges funding through a PLS fellowship from the Gordon and Betty Moore foundation. JS is funded by a Project Grant from the Swedish Research Council (2015-05449). MEC is funded by the Royal Society. This work was funded in part by EPSRC Grant EP/J007404. YK is supported by an I-CORE Program of the Planning and Budgeting Committee of the Israel Science Foundation and an Israel Science Foundation grant. JT is funded by ANR Baccterns.

[1] M. Ballerini, N. Cabibbo, R. Candelier, A. Cavagna, E. Cisbani, I. Giardina, V. Lecomte, A. Orlandi, G. Parisi, A. Procaccini, *et al.*, Proceedings of the National Academy of Sciences USA **105**, 1232 (2008).
[2] V. Schaller, C. Weber, C. Semmrich, E. Frey, and A. R. Bausch, Nature **467**, 73 (2010).
[3] Y. Sumino, K. H. Nagai, Y. Shitaka, D. Tanaka, K. Yoshikawa, H. Chaté, and K. Oiwa, Nature **483**, 448 (2012).
[4] H. H. Wensink, J. Dunkel, S. Heidenreich, K. Drescher, R. E. Goldstein, H. Löwen, and J. M. Yeomans, Proceedings of the National Academy of Sciences USA **109**, 14308 (2012).
[5] M. Marchetti, J. Joanny, S. Ramaswamy, T. Liverpool, J. Prost, M. Rao, and R. A. Simha, Reviews of Modern Physics **85**, 1143 (2013).
[6] A. Bricard, J.-B. Caussin, N. Desreumaux, O. Dauchot, and D. Bartolo, Nature **503**, 95 (2013).
[7] W. F. Paxton, K. C. Kistler, C. C. Olmeda, A. Sen, S. K. St. Angelo, Y. Cao, T. E. Mallouk, P. E. Lammert, and V. H. Crespi, Journal of the American Chemical Society **126**, 13424 (2004).
[8] J. Deseigne, O. Dauchot, and H. Chaté, Physical Review Letters **105**, 098001 (2010).
[9] J. Palacci, C. Cottin-Bizonne, C. Ybert, and L. Bocquet, Physical Review Letters **105**, 088304 (2010).
[10] S. Thutupalli, R. Seemann, and S. Herminghaus, New Journal of Physics **13**, 073021 (2011).
[11] I. Buttinoni, J. Bialké, F. Kümmel, H. Löwen, C. Bechinger, and T. Speck, Physical Review Letters **110**, 238301 (2013).
[12] J. Stenhammar, R. Wittkowski, D. Marenduzzo, and M. E. Cates, Science Advances **2** (2016).
[13] M. E. Cates and J. Tailleur, Annual Review of Condensed Matter Physics **6**, 219 (2015).
[14] J. Tailleur and M. Cates, Physical Review Letters **100**, 218103 (2008).
[15] A. Thompson, J. Tailleur, M. Cates, and R. Blythe, Journal of Statistical Mechanics: Theory and Experiment **2011**, P02029 (2011).
[16] Y. Fily and M. C. Marchetti, Physical Review Letters **108**, 235702 (2012).
[17] G. S. Redner, M. F. Hagan, and A. Baskaran, Physical Review Letters **110**, 055701 (2013).
[18] J. Bialké, H. Löwen, and T. Speck, EPL (Europhysics Letters) **103**, 30008 (2013).
[19] J. Stenhammar, A. Tiribocchi, R. J. Allen, D. Marenduzzo, and M. E. Cates, Physical Review Letters **111**, 145702 (2013).
[20] A. Wysocki, R. G. Winkler, and G. Gompper, EPL (Europhysics Letters) **105**, 48004 (2014).
[21] I. Theurkauff, C. Cottin-Bizonne, J. Palacci, C. Ybert, and L. Bocquet, Physical Review Letters **108**, 268303 (2012).
[22] R. Wittkowski, A. Tiribocchi, J. Stenhammar, R. J. Allen, D. Marenduzzo, and M. E. Cates, Nature Communications **5** (2014).
[23] S. C. Takatori, W. Yan, and J. F. Brady, Physical Review Letters **113**, 028103 (2014).
[24] T. Speck, J. Bialké, A. M. Menzel, and H. Löwen, Physical Review Letters **112**, 218304 (2014).
[25] R. Matas-Navarro, R. Golestanian, T. B. Liverpool, and S. M. Fielding, Physical Review E **90**, 032304 (2014).
[26] A. Zöttl and H. Stark, Physical Review Letters **112**, 118101 (2014).
[27] A. Suma, G. Gonnella, D. Marenduzzo, and E. Orlandini, EPL (Europhysics Letters) **108**, 56004 (2014).
[28] A. P. Solon, J. Stenhammar, R. Wittkowski, M. Kardar, Y. Kafri, M. E. Cates, and J. Tailleur, Physical Review Letters **114**, 198301 (2015).
[29] M. J. Schnitzer, Physical Review E **48**, 2553 (1993).
[30] C. Liu, X. Fu, L. Liu, X. Ren, C. K. Chau, S. Li, L. Xiang, H. Zeng, G. Chen, L.-H. Tang, *et al.*, Science **334**, 238 (2011).
[31] R. Soto and R. Golestanian, Physical Review E **89**, 012706 (2014).
[32] M. Cates and J. Tailleur, EPL (Europhysics Letters) **101**, 20010 (2013).
[33] A. P. Solon, Y. Fily, A. Baskaran, M. Cates, Y. Kafri, M. Kardar, and J. Tailleur, Nature Physics **11**, 673 (2015).
[34] X. Yang, M. L. Manning, and M. C. Marchetti, Soft Matter **10**, 6477 (2014).
[35] S. C. Takatori and J. F. Brady, Physical Review E **91**, 032117 (2015).
[36] Equation (1) is generic if M is allowed to include gradient terms that will not play any role in the following.
[37] This would also be required to study equilibrium phase separation and only means that we consider macroscopic phases for which the Laplace pressure is negligible.
[38] For example, in flow-induced phase separation (shear banding) the composition of coexisting phases alters as one traverses the tie-line by increasing the mean shear rate; see [43].
[39] J. W. Cahn and J. E. Hilliard, The Journal of chemical physics **28**, 258 (1958).

[40] See Supplemental Material [url], which includes Refs. XXX.
[41] C. Kipnis and C. Landim, *Scaling limits of interacting particle systems*, Vol. 320 (Springer Science & Business Media, 2013).
[42] A. Solon, M. Cates, and J. Tailleur, The European Physical Journal Special Topics **224**, 1231 (2015).
[43] S. M. Fielding and P. D. Olmsted, The European Physical Journal E **11**, 65 (2003).
[44] M. Mijalkov, A. McDaniel, J. Wehr, and G. Volpe, Phys. Rev. X **6**, 011008 (2016).
[45] F. Farrell, M. Marchetti, D. Marenduzzo, and J. Tailleur, Physical Review Letters **108**, 248101 (2012).
[46] K. Binder, Reports on progress in physics **50**, 783 (1987).
[47] E. Bertin, O. Dauchot, and M. Droz, Physical Review Letters **96**, 120601 (2006).
[48] E. Bertin, K. Martens, O. Dauchot, and M. Droz, Physical Review E **75**, 031120 (2007).
[49] R. Dickman, New Journal of Physics **18**, 043034 (2016).